inorganics

MDPI

Article

Effect of CaO/SiO_2 and MgO/Al_2O_3 on the Metallurgical Properties of Low Boron-Bearing High-Alumina Slag

Ye Sun [1,2], Zuoliang Zhang [1,2,*], Chunlei Wu [1,2] and Zhenggen Liu [3]

[1] Liaoning Key Laboratory of Optimization and Utilization of Non-Associated Low-Grade Iron Ore, Liaoning Institute of Science and Technology, Benxi 117004, China
[2] School of Metallurgy and Materials Engineering, Liaoning Institute of Science and Technology, Benxi 117004, China
[3] School of Metallurgy, Northeastern University, Shenyang 110819, China
* Correspondence: zhang231167@163.com

Abstract

For optimizing the operational efficiency and productivity within blast furnace processes, a profound understanding of the viscous flow characteristics of $CaO–SiO_2–MgO–Al_2O_3–B_2O_3$ slag systems is of paramount importance. In this study, we conducted a comprehensive investigation into the influence of the CaO/SiO_2 and MgO/Al_2O_3 ratios on the viscosity, break point temperature (T_{Br}), and activation energy (E_η) of low boron-bearing high-alumina slag. Concurrently, we elucidated the underlying mechanisms through which these ratios affect the viscous behavior of the slag by employing a combination of analytical techniques, including X-Ray Diffraction (XRD), Fourier Transform Infrared Spectroscopy (FTIR), and thermodynamic modeling using the Factsage software. The experimental findings reveal that, as the CaO/SiO_2 ratio increases from 1.10 to 1.30, the slag viscosity at 1773 K decreases from 0.316 Pa·s to 0.227 Pa·s, while both the T_{Br} and E_η exhibit an upward trend, rising from 1534 K and 117.01 kJ·mol^{-1} to 1583 K and 182.86 kJ·mol^{-1}, respectively. Conversely, an elevation in the MgO/Al_2O_3 ratio from 0.40 to 0.65 results in a reduction in slag viscosity at 1773 K from 0.290 Pa·s to 0.208 Pa·s, accompanied by a decrease in T_{Br} from 1567 K to 1542 K. The observed deterioration in slag flow properties can be attributed to an enhanced polymerization degree of complex viscous structural units within the slag matrix. Ultimately, our study identifies that an optimal viscous performance of the slag is achieved when the CaO/SiO_2 ratio is maintained at 1.25 and the MgO/Al_2O_3 ratio is maintained at 0.55, providing valuable insights for the rational design and control of blast furnace slag systems.

Keywords: high-alumina slag; viscous behavior; activation energy; slag structure; MgO/Al_2O_3; CaO/SiO_2

check for updates

Academic Editor: Aivaras Kareiva

Received: 10 September 2025
Revised: 17 October 2025
Accepted: 20 October 2025
Published: 24 October 2025

Citation: Sun, Y.; Zhang, Z.; Wu, C.; Liu, Z. Effect of CaO/SiO_2 and MgO/Al_2O_3 on the Metallurgical Properties of Low Boron-Bearing High-Alumina Slag. *Inorganics* **2025**, *13*, 346. https://doi.org/10.3390/inorganics13110346

Copyright: © 2025 by the authors. Licensee MDPI, Basel, Switzerland. This article is an open access article distributed under the terms and conditions of the Creative Commons Attribution (CC BY) license (https://creativecommons.org/licenses/by/4.0/).

1. Introduction

The cost-reduction and economic–efficiency-enhancement strategies for ironmaking enterprises frequently involve the utilization of low-cost bentonite and high-alumina ores in blast furnace smelting processes. However, excessive Al_2O_3 content in slag can induce detrimental effects, including elevated slag viscosity, impaired permeability in the cohesive zone, and compromised slag–iron separation efficiency. While B_2O_3 incorporation has been validated to improve slag viscous behavior, the addition of CaO and MgO mitigates slag polymerization through network depolymerization, thereby enhancing flowability [1]. Excessive CaO/MgO, however, escalates slag volume and energy consumption, conflicting

with energy conservation and emission reduction goals. Consequently, systematic investigation of CaO/SiO_2 and MgO/Al_2O_3 ratios on viscous flow characteristics in low-boron high-alumina slag systems is imperative [2,3].

Recent studies have advanced the understanding of boron-containing slag rheology. Li et al. [4] demonstrated that, in $CaO–MgO–Al_2O_3–SiO_2$-10 wt% FeO systems (C/S = 1.4), MgO promotes silicate network depolymerization and viscosity reduction, whereas Al_2O_3 > 10 wt% induces counteracting polymerization effects. Liang et al. [5] reported that increasing CaO/SiO_2 from 1.10 to 1.30 reduces slag polymerization degree, viscosity (η), activation energy (E_η), and break temperature (T_{Br}), while MgO content elevation (6.0–12.0 wt%) exhibits non-monotonic effects on η, T_{Br}, and E_η. Gao et al. [6] observed that viscosity in $SiO_2–CaO–MgO$-9 wt% Al_2O_3 systems (basicity 0.4–1.0; MgO 13–19 wt%) depends on the synergistic action of basic oxides, with basicity elevation being more effective than MgO increase in viscosity reduction at lower temperatures. Huang et al. [7] confirmed that B_2O_3 incorporation in SiO_2-30 wt% $Al_2O_3–B_2O_3$-12 wt% $Na_2O–CaO$ systems reduces polymerization degree, viscosity, and T_{Br}. Despite these advances, the combined effects of CaO/SiO_2 and MgO/Al_2O_3 ratios on low-boron high-alumina slag viscous behavior remain underexplored.

This study systematically investigates the influence of CaO/SiO_2 and MgO/Al_2O_3 ratios on the viscous flow characteristics of low-boron high-alumina slag, with a focus on viscosity, break temperature, and viscous flow activation energy. Experimental viscosity measurements were conducted across a range of slag compositions. Mechanistic insights were elucidated through X-Ray Diffraction (XRD) and Fourier-Transform Infrared Spectroscopy (FTIR) analyses, while Factsage (version 7.2) thermodynamics software was employed to determine liquidus temperatures. The optimal slag composition identified herein provides theoretical guidance for industrial practice in ironmaking enterprises.

2. Results and Discussion

Different CaO/SiO_2 and MgO/Al_2O_3 slag were obtained through experiments. The $\eta–T$ curve is shown in Figure 1. The viscosity increases with decreasing temperature, and there is a clear turning point on every $\eta–T$ curve.

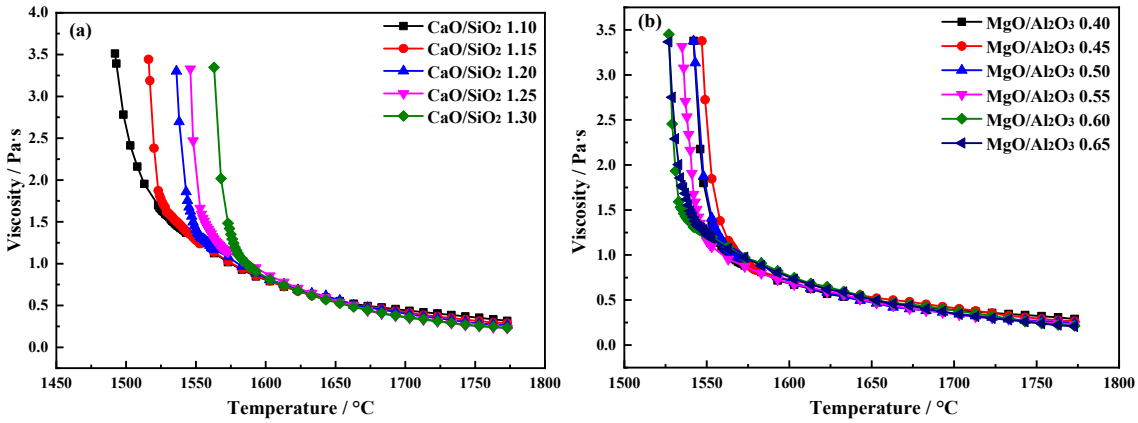


Figure 1. $\eta–T$ curves of experimental slags with different CaO/SiO_2 and MgO/Al_2O_3. (**a**)—CaO/SiO_2; (**b**)—MgO/Al_2O_3.

2.1. Effects of CaO/SiO_2 and MgO/Al_2O_3 on the Viscous Behaviors of the Slag

2.1.1. Effects of CaO/SiO_2 on the Viscous Behaviors of the Slag

The effects of different CaO/SiO_2 on slag viscosity are shown in Figure 2a. When the temperature increases from 1733 to 1773 K, with an increase in CaO/SiO_2 from 1.10 to 1.30,

the η of the slag decreases significantly first and then slows down. When CaO/SiO_2 is 1.25, the minimum of η_{1773K} is 0.227 Pa·s.

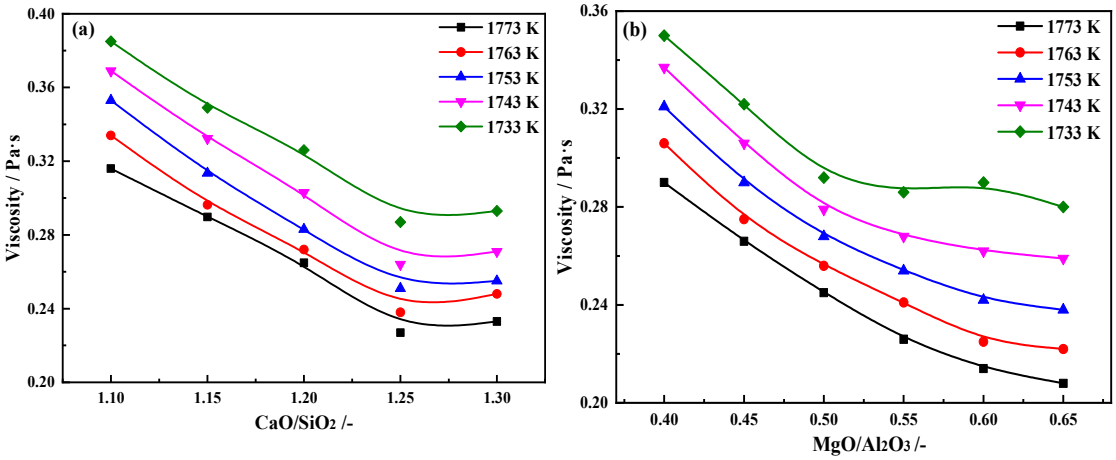


Figure 2. Viscosity of different CaO/SiO_2 and MgO/Al_2O_3 experimental slags at 1733–1773 K. (**a**)—CaO/SiO_2; (**b**)—MgO/Al_2O_3.

The viscosity of slag is mainly affected by the internal network structure. The $Si_xO_y^{z-}$ and $Al_xO_y^{z-}$ tetrahedral structures are the main structural units of the slag. The complex network structure inside the slag can be depolymerized to reduce viscosity. As CaO/SiO_2 increases in the slag, the viscosity will decrease. The reason is that the free oxygen ion O^{2-} dissociated from basic oxide CaO can interact with bridging oxygen O in the network structure of aluminosilicate to form non-bridging oxygen O^- [8–10], resulting in the aluminate silicate network structure being depolymerized into smaller network units. By the viscosity module of FactSage prediction, the theoretical viscosities at 1773 K are 0.314, 0.296, 0.281, 0.268, and 0.256 Pa·s, respectively. The trend of change is the same as that of the experiment, providing theoretical support for the experimental results.

In order to elucidate the relationship between slag viscosity and internal structure, FTIR is employed to analyze the slag of different CaO/SiO_2. The FTIR of silicate aluminate slag is generally divided into three regions, and the wave number range is 400–600 cm^{-1}, 600–800 cm^{-1}, and 800–1200 cm^{-1}, which respectively corresponds to T–O–T (T represents Si or Al) bending vibration, $[AlO_4]^{5-}$ tetrahedral asymmetric tensile vibration, and $[SiO_4]^{4-}$ tetrahedral symmetric tensile vibration [11–13]. The FTIR analysis results of different CaO/SiO_2 are shown in Figure 3a. As CaO/SiO_2 increases from 1.10 to 1.30, the transmitted wave valley of the $[SiO_4]^{4-}$ tetrahedral symmetric stretching vibration band shifts towards lower wave numbers, and the bandwidth widens, indicating the simplification of the aluminosilicate network structure. Gaussian deconvolution was performed on Si–O axisymmetric vibration bands with CaO/SiO_2 ratios of 1.10 and 1.30, and the corresponding areas of each peak are used to characterize the corresponding amount of Q_i (i = 0~3). Q_0, Q_1, Q_2, and Q_3 represent the structures of SiO_4^{4-}, $Si_2O_7^{6-}$, $Si_2O_6^{4-}$, and $Si_2O_5^{2-}$ [14–16]. The smaller the value of i, the simpler is the slag structure, and the higher is the degree of polymerization. In brief, when CaO/SiO_2 increases from 1.10 to 1.30, the silicate and aluminate network structure in the slag are depolymerized, resulting in the reduction in the η in the slag.

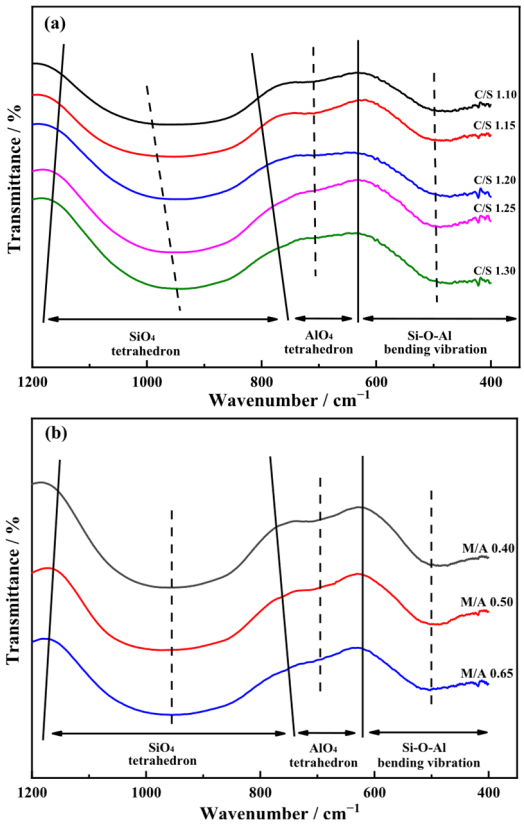


Figure 3. FTIR of experimental slag with different CaO/SiO_2 and MgO/Al_2O_3. (**a**)—CaO/SiO_2; (**b**)—MgO/Al_2O_3.

2.1.2. Effects of MgO/Al_2O_3 on the Viscous Behaviors of the Slag

The effects of different MgO/Al_2O_3 on slag viscosity are shown in Figure 2b. When the temperature increases from 1733 to 1773 K, with an increase in CaO/SiO_2 from 0.40 to 0.65, the η of the slag decreases significantly first and then slows down. When MgO/Al_2O_3 is 0.55, the η_{1773K} is 0.226 Pa·s.

The effect mechanism of MgO/Al_2O_3 on slag viscosity is similar to the CaO/SiO_2. Both MgO and CaO are basic oxide, and the dissociated O^{2-} ions promote the depolymerization of complex structures. By the viscosity module of FactSage prediction, when MgO/Al_2O_3 increases from 0.40 to 0.65, the theoretical viscosities at 1773 K are 0.281, 0.272, 0.263, 0.254, 0.247, and 0.239 Pa·s, respectively. The trend of change is the same as that of the experiment, providing theoretical support for the experimental results.

In order to elucidate the relationship between slag viscosity and internal structure, FTIR is employed to analyze the slag of different MgO/Al_2O_3. The FTIR analysis results of different MgO/Al_2O_3 slag are shown in Figure 3b. When MgO/Al_2O_3 increases from 0.40 to 0.65, the depth of $[SiO_4]^{4-}$ tetrahedral symmetric tensile vibration becomes shallower, and the bandwidth becomes wider, indicating an increase in the distance between Si–O bonds and the disintegration of the slag silicate network structure into smaller network units; the depth of the $[AlO_4]^{5-}$ tetrahedron asymmetric tensile vibration band gradually becomes shallow and finally almost disappears, indicating the aluminate network structure in the slag is depolymerized; and the groove depth of the Si–O–Al bending vibration band is slightly weakened, indicating a decrease in the number of Si–O–Al structures used to connect $[AlO_4]^{5-}$ and $[SiO_4]^{4-}$ tetrahedra [17–19]. In conclusion, the silicon aluminate network structure in the slag is depolymerized, resulting in the reduction in the η in the slag.

2.2. Effects of CaO/SiO_2 and MgO/Al_2O_3 on the Break Point Temperature of Slag

2.2.1. Effects of CaO/SiO_2 on the Break Point Temperature of Slag

The effect of different CaO/SiO_2 on the break point temperature is shown in Figure 4a. When CaO/SiO_2 increases from 1.10 to 1.30, the T_{Br} shows an uptrend, increasing from 1534 K to 1583 K.

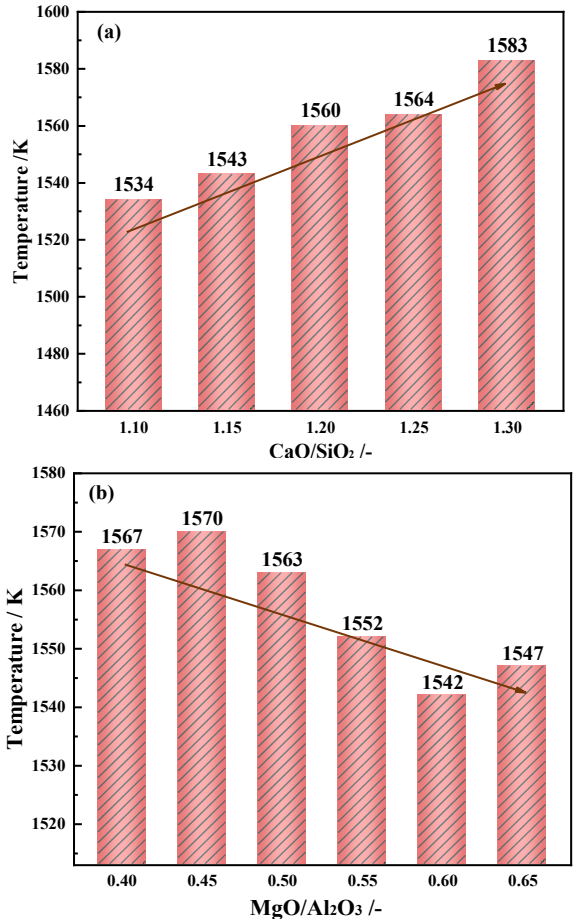


Figure 4. T_{Br} of experimental slags with different CaO/SiO_2 and MgO/Al_2O_3. (**a**)—CaO/SiO_2; (**b**)—MgO/Al_2O_3.

The phase diagram of the five-component slag system $CaO–SiO_2–MgO$-17.00%Al_2O_3-3.83%B_2O_3 as plotted by the phase diagram module in the FactSage is shown in Figure 5. The different CaO/SiO_2 components are located in the crystalline region of the pyrochlore. With the increase in CaO/SiO_2, the liquid temperature of the slag increases, and the ability to crystallize at high temperatures becomes stronger, leading to an increase in T_{Br}. The liquid temperatures were 1613.92, 1623.05, 1631.00, 1637.96, and 1643.76 K, respectively. The liquidus temperature of the slag increased. Thus, the crystallization capacity of the slag is enhanced, and the T_{Br} also increases. These results are in agreement with the trend of the measurements of T_{Br}.

The XRD analysis results of different CaO/SiO_2 slag are shown in Figure 6a. The basic phase in different CaO/SiO_2 slag is melilite. When CaO/SiO_2 increases from 1.10 to 1.30, the diffraction peak intensity of melilite, spinel, and $Ca_2B_2O_5$ phases increases. When CaO/SiO_2 is 1.15, the $Mg_3(BO_3)_2$ phase disappears, and the pyroxene phase appears in the slag. The number of high melting point phases in the slag increases relatively, and the crystallization ability of the slag increases under high temperature conditions, resulting in an increase in the T_{Br} and a decrease in fluidity.

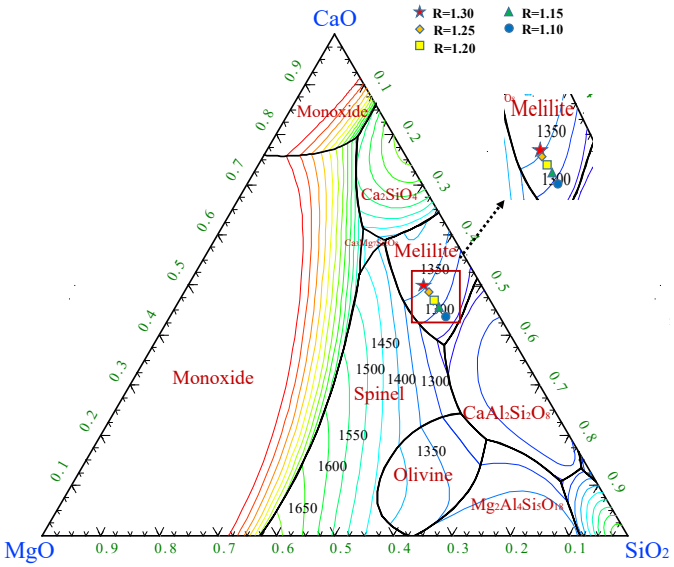


Figure 5. Phase diagram of CaO–SiO_2–MgO-17.00%Al_2O_3-0.47%B_2O_3 blast furnace slag with different CaO/SiO_2.

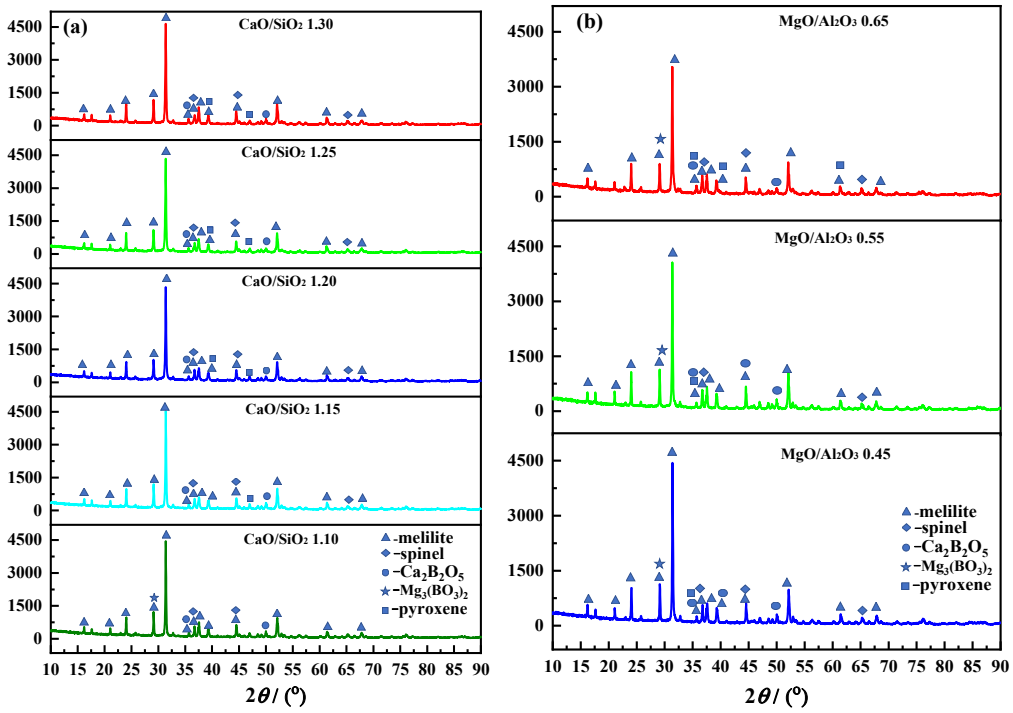


Figure 6. XRD analysis of different CaO/SiO_2 and MgO/Al_2O_3 experimental slags. (**a**)—CaO/SiO_2; (**b**)—MgO/Al_2O_3.

2.2.2. Effects of MgO/Al_2O_3 on the Break Point Temperature of Slag

The effect of different MgO/Al_2O_3 on the break point temperature is shown in Figure 4b. With the increasing of MgO/Al_2O_3 from 0.40 to 0.65, the T_{Br} of the slag shows a downward trend, decreasing from 1570 K to 1542 K.

The phase diagram of the CaO–SiO_2-7.98%MgO–Al_2O_3-0.47%B_2O_3 slag system is calculated by the Phase Diagram module in FactSage. As shown in Figure 7, with the continuous decrease in MgO/Al_2O_3, the composition of the slags is located in the area of the melilite phase, and the liquidus temperature of melilite is relatively sparse, which demonstrates that the phase is stable. According to FactSage, the liquidus temperature of slag with different MgO/Al_2O_3 was calculated as 1345.83, 1349.95, 1354.95, 1360.93, 1367.64,

and 1374.78 °C, and the liquidus temperature of the slag increased. Thus, the crystallization capacity of the slag is enhanced, and the T_{Br} also increases. These results are in agreement with the trend of the measurements of T_{Br}.

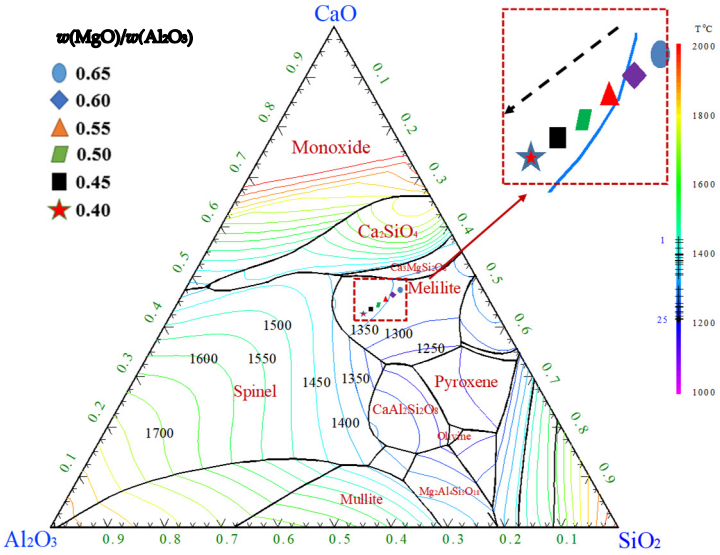


Figure 7. Phase diagram of five-element slag system CaO–SiO_2-7.98%MgO–Al_2O_3-0.47%B_2O_3 with different MgO/Al_2O_3.

The XRD analysis results of different MgO/Al_2O_3 slag are shown in Figure 6b. There are melilite, spinel, pyroxene, $Ca_2B_2O_5$, and $Mg_3(BO_3)_2$ in the slag, and the melilite is the basic phase. When MgO/Al_2O_3 increases from 0.40 to 0.65, the diffraction peak intensity of melilite, spinel, pyroxene, and $Mg_3(BO_3)_2$ gradually weakens, while the diffraction peak intensity of $Ca_2B_2O_5$ and pyroxene slightly increases. This indicates that the $Ca_2B_2O_5$ and pyroxene in the slag are relatively increased, while the number of high melting point phases is relatively reduced, resulting in a decrease in the crystallization ability of the slag, a decrease in the T_{Br}, and an improvement in fluidity under high temperature conditions.

2.3. Effects of CaO/SiO_2 and MgO/Al_2O_3 on Activation Energy of Slag Viscous Flow

Viscous flow activation energy is a crucial viscosity characteristic of slag. The E_η reflects the sensitivity of slag viscosity to temperature, representing the thermostability of slag [20–22]. The calculation of viscous flow activation energy in this article adopts the modified Weymann–Frenkel equation by Urban, as shown in Formula (1). Formula (2) can be obtained by taking the logarithm of both sides of Formula (1). The viscosity data measured in the experiment are calculated using the linear regression method, and the slope is E_η. The linear fitting results and the trend of E_η with different CaO/SiO_2 and MgO/Al_2O_3 are shown in Figure 8. The results indicate that there is a fine linear relationship between $\ln(\eta/T)$ and $1/T$. The linear correlation coefficients are all greater than 0.99 [23,24].

$$\eta = ATexp\left(\frac{E_\eta}{RT}\right) \quad (1)$$

$$\ln\left(\frac{\eta}{T}\right) = \ln A + \frac{E_\eta}{R} \times \frac{1}{T} \quad (2)$$

where η is the viscosity, Pa·s; A is the proportionality constant; T is the temperature, K; and R is the gas constant, 8.314 J·(mol·K)$^{-1}$.

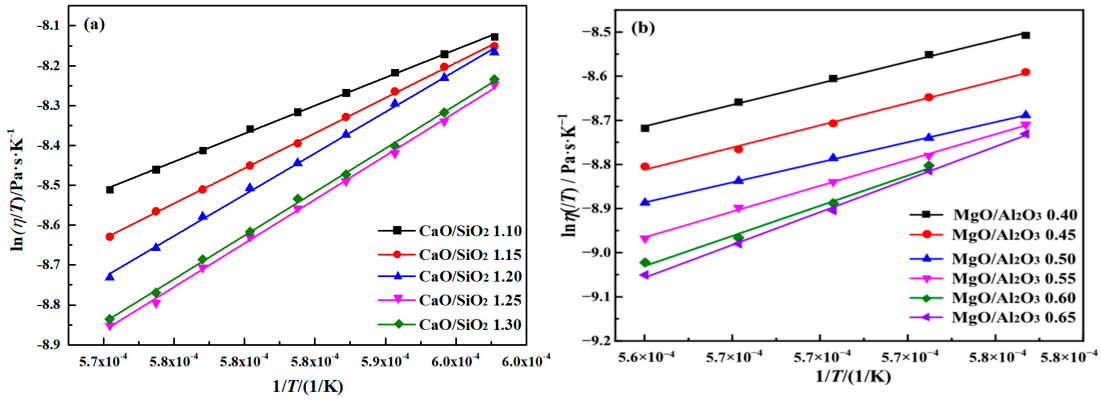


Figure 8. Fitting results of experimental slag $\ln(\eta/T)$ and $1/T$ for different CaO/SiO_2 and MgO/Al_2O_3. (**a**)—CaO/SiO_2; (**b**)—MgO/Al_2O_3.

2.3.1. Effects of CaO/SiO_2 on Activation Energy of Slag Viscous Flow

As shown in Figure 9a, when CaO/SiO_2 increases from 1.10 to 1.30, the E_η increases from 117.01 to 182.86 kJ·mol^{-1}. This indicates that the sensitivity of slag viscosity to temperature is weakened. On the premise of ensuring better slag stability, the CaO/SiO_2 value of 1.25 is reasonable. From the perspective of slag structure, the complex slag structure is decomposed into a simpler structure, the activation energy of slag is increased, and the stability is improved [25–27]. The stability of the slag can also be characterized by the density of the isotherm in the phase diagram. The thinner the contour lines temperature and related subjects, the less the temperature affects the slag composition, and the better the slag stability is.

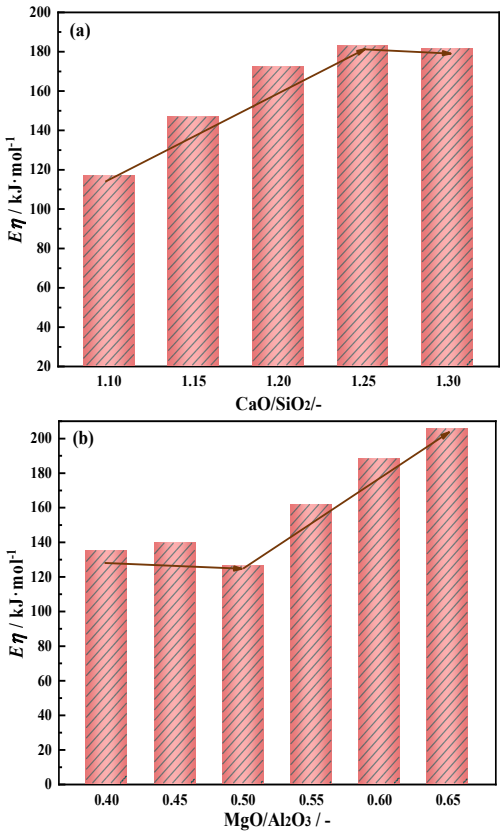


Figure 9. Variation in E_η for different CaO/SiO_2 and MgO/Al_2O_3 experimental slags. (**a**)—CaO/SiO_2; (**b**)—MgO/Al_2O_3.

2.3.2. Effects of MgO/Al_2O_3 on Activation Energy of Slag Viscous Flow

As shown in Figure 9b, when MgO/Al_2O_3 increases from 0.40 to 0.50, the E_η changes inconspicuously. The E_η increases from 126.20 to 205.86 kJ·mol^{-1}. When MgO/Al_2O_3 increases from 0.50 to 0.65, the E_η significantly increases. This indicates that the thermostability of the slag to temperature is enhanced. The complex slag structure is decomposed into a simpler structure, and the activation energy of the slag is increased.

As shown in Figures 6 and 8, within the experimental value range, the isotherm becomes sparse with the increase in CaO/SiO_2 and MgO/Al_2O_3, indicating a better stability of the slag, which is consistent with the experimental fitting results [28,29].

Briefly, when CaO/SiO_2 is 1.25, η_{1773K} has a minimum of 0.227 Pa·s, the T_{Br} is lower at 1570 K, E_η is stable at a lower level, and the slag has a good thermal stability performance. When MgO/Al_2O_3 is 0.55, the decreasing trend of η_{1773K} begins to slow down to 0.226 Pa·s, and T_{Br} and E_η are 1570 K and 161.99 KJ·mol^{-1}, respectively. Overall, when CaO/SiO_2 is 1.25 and MgO/Al_2O_3 is 0.55, good metallurgical properties of the low boron-bearing high-alumina slag system can be obtained, providing a good reference basis for blast furnace operation.

3. Experimental

3.1. Raw Material

Based on the on-site BF slag compositions, the slag samples for the experiments were synthesized with the analytical reagent oxides of CaO, SiO_2, MgO, and Al_2O_3. The basicity of the BF slag is 1.25, the Al_2O_3 is 17.00%, the B_2O_3 is 0.47%, and the MgO/Al_2O_3 is 0.47, which belongs to the boron-bearing high-alumina blast furnace slag. The chemical compositions of the slag samples are listed in Table 1. The experimental slag samples were synthesized by adding the analytical-grade oxides, with the site blast furnace slag as the reference slag. In order to improve the accuracy of the experiment, the furnace slag and the analytical-grade oxides were roasted, mixed evenly, put into the molybdenum crucible, and then pre-melted under an argon atmosphere to stabilize the temperature and homogenize the compositions. The pre-melted slag samples were used for the determination of viscous flow behaviors [30]. The experimental scheme is shown in Table 2. In series-1, MgO was kept at 7.98%, Al_2O_3 was kept at 17.00%, and B_2O_3 was kept at 0.47% in the slag, and CaO/SiO_2 was increased from 1.10 to 1.30. In series-2, CaO/SiO_2 ratio was kept at 1.25 in the slag, and MgO/Al_2O_3 was increased from 0.40 to 0.65.

Table 1. Chemical composition of base blast furnace slag (mass fraction/%).

CaO	SiO_2	MgO	Al_2O_3	B_2O_3
38.01	30.37	7.98	17.00	0.47

Table 2. Experimental scheme (mass fraction/%).

No.	CaO	SiO_2	MgO	Al_2O_3	B_2O_3	CaO/SiO_2	MgO/Al_2O_3
1	35.03	31.85	7.98	17.00	0.47	1.10	0.47
2	35.77	31.11	7.98	17.00	0.47	1.15	0.47
3	36.48	30.40	7.98	17.00	0.47	1.20	0.47
4	37.15	29.72	7.98	17.00	0.47	1.25	0.47
5	37.80	29.08	7.98	17.00	047	1.30	0.47
6	37.81	30.25	6.80	17.00	0.47	1.25	0.40
7	37.74	29.87	7.65	17.00	0.47	1.25	0.45
8	36.87	29.49	8.50	17.00	0.47	1.25	0.50
9	36.39	29.11	9.35	17.00	0.47	1.25	0.55
10	35.92	28.74	10.20	17.00	0.47	1.25	0.60
11	35.45	28.36	11.05	17.00	0.47	1.25	0.65

3.2. Experimental Procedure

The viscosity–temperature (η–T) curves of the slag were acquired on an RTW-10 melt property tester by the rotating cylinder method. Figure 10 shows the schematic diagram of the experimental device, which consisted of a heating system, a rotating system, a measuring system, a control system, and an atmosphere system.

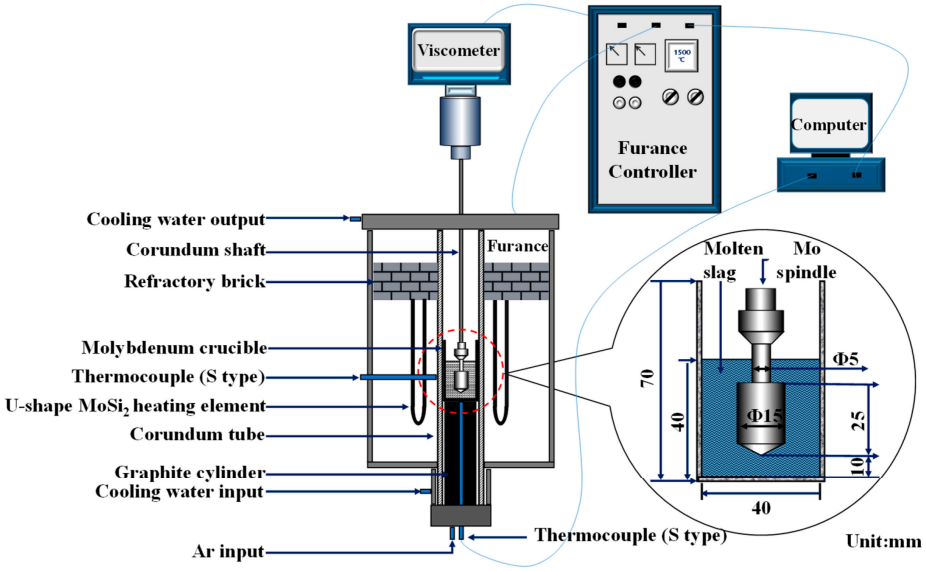


Figure 10. Schematic diagram of the experimental apparatus.

The crucible containing the experimental slag sample was placed on a graphite base and heated to 1500 °C with the furnace temperature, and then, the temperature was held for 30 min. During the constant temperature, a molybdenum probe was used to stir the slag to homogenize the chemical compositions. When the temperature stabilized, the viscosity was measured at a speed of 200 r/min. In the process of viscosity measurement, argon gas was injected into the furnace tube at a flow rate of 1.5 L/min to maintain an inert atmosphere. The measurement results were recorded by the control system. When the viscosity reached about 3.5 Pa·s, the measurements were ended. The experiment was repeated twice. The quenched experimental slags and the natural cooling slags were crushed and grinded to facilitate the analysis by FTIR and XRD (Bruker D8 ADVANCE, Karlsruhe, Gemany).

This article defines the viscosity of slag at 1773 K as high-temperature viscosity (η_{1773K}). Making 135° straight line is tangent to the viscosity–temperature curve(η–T). The temperature corresponding to the tangent point is defined as the T_{Br} of the slag, as shown in Figure 11.

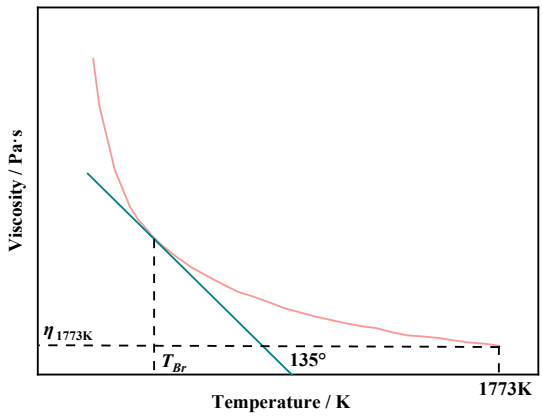


Figure 11. Slag viscosity curve and T_{Br} determination diagram.

4. Conclusions

(1) With CaO/SiO_2 increasing from 1.10 to 1.30, viscosity first decreased significantly and then slowed down. When CaO/SiO_2 is 1.25, η_{1773K} is 0.227 Pa·s. T_{Br} shows an increasing trend, increasing from 1534 K to 1583 K. E_η increases from 117.01 to 182.86 kJ·mol^{-1}, and the thermal stability of the slag deteriorates first and then improves. At this point, the slag system has a better performance.

(2) With MgO/Al_2O_3 increasing from 0.40 to 0.65, viscosity first decreased significantly and then slowed down. When MgO/Al_2O_3 is 0.55, η_{1773K} is 0.226 Pa·s. T_{Br} decreases from 1570 K to 1542 K. The E_η increases from 126.20 to 205.86 kJ·mol^{-1}, and the thermal stability of the slag first improves and then deteriorates. At this point, the slag system has a better performance.

(3) For comprehensive considerations, when CaO/SiO_2 is 1.25 and MgO/Al_2O_3 is 0.55, the η_{1773K}, T_{Br}, and E_η are at a reasonable value. The low boron-bearing high-alumina slag system has the best metallurgical performance at this value.

Author Contributions: Y.S.: Investigation, Writing—original draft. Z.Z.: Writing—review and editing. C.W.: Data curation, Photo editing. Z.L.: Methodology, Validation.. All authors have read and agreed to the published version of the manuscript.

Funding: This research was funded by the Technological Project in Liaoning (2022JH2/101300124) and Basic Research Project of Education Department of Liaoning Province (2024JYTKYTD-16).

Institutional Review Board Statement: Not applicable.

Informed Consent Statement: Not applicable.

Data Availability Statement: The original contributions presented in this study are included in the article. Further inquiries can be directed to the corresponding author.

Acknowledgments: The authors are especially grateful to the Technological Project in Liaoning (2022JH2/101300124) and Basic Research Project of Education Department of Liaoning Province (2024JYTKYTD-16).

Conflicts of Interest: The authors declare that they have no known competing financial interests or personal relationships that could have appeared to influence the work reported in this paper.

References

1. Zhang, X.Y.; Wang, S.Z.; Zhao, J.; Wu, Z.; Geng, Y.; Ma, Y.; Xue, R. Influence of B_2O_3 on the thermophysical properties of molten blast furnace slag. *J. Non-Cryst. Solids* **2023**, *615*, 122429. [CrossRef]
2. Bi, Z.; Li, K.; Jiang, C.; Zhang, J.; Ma, S.; Sun, M.; Wang, Z.; Li, H. Effects of B_2O_3 on the structure and properties of blast furnace slag by molecular dynamics simulation. *J. Non-Cryst. Solids* **2021**, *551*, 120412. [CrossRef]
3. Talapaneni, T.; Chaturvedi, V. Proposing a suitable slag composition by estimating the fusion behavior, viscosity and desulphurization ability for blast furnaces running with high alumina. *Mater. Today Proc.* **2022**, *67*, 558–565. [CrossRef]
4. Li, T.; Zhao, C.; Sun, C.; Song, S.; Wang, Q. Roles of MgO and Al_2O_3 in viscous and structural behavior of blast furnace primary slag with C/S = 1.4. *Metall. Mater. Trans. B* **2020**, *51*, 2724–2734. [CrossRef]
5. Liang, H.L.; Chu, M.S.; Feng, C.; Tang, J.; Liu, Z.; Wang, W. Optimisation study and affecting mechanism of CaO/SiO_2 and MgO on viscous behaviours of titanium-bearing blast furnace slag. *Ironmak. Steelmak.* **2018**, *47*, 106–117. [CrossRef]
6. Gao, Y.; Wang, S.; Hong, C.; Ma, X.J.; Yang, F. Effects of basicity and MgO content on the viscosity of the SiO_2-CaO-MgO-9wt%Al_2O_3 slag system. *Int. J. Miner. Metall. Mater.* **2014**, *21*, 353–362. [CrossRef]
7. Huang, X.H.; Liao, J.L.; Zheng, K.; Hu, H.H.; Wang, F.M.; Zhang, Z.T. Effect of B_2O_3 addition on viscosity of mould slag containing low silica content. *Ironmak. Steelmak.* **2014**, *41*, 67–74. [CrossRef]
8. Sukenaga, S.; Higo, T.; Shibata, H.; Saito, N. Effect of CaO/SiO_2 ratio on surface tension of CaO-SiO_2-Al_2O_3-MgO Melts. *ISIJ Int.* **2015**, *55*, 1299–1304. [CrossRef]
9. Saito, N.; Hori, N.; Nakashima, K.; Mori, K. Viscosity of blast furnace type slags. *Metall. Mater. Trans. B* **2003**, *34*, 509–516. [CrossRef]

10. Jiang, C.; Li, K.; Zhang, J.; Qin, Q.; Liu, Z.; Liang, W.; Sun, M. Molecular dynamics simulation on the effect of MgO/Al_2O_3 ratio on structure and properties of blast furnace slag under different basicity conditions. *Metall. Mater. Trans. B* **2018**, *50*, 367–375. [CrossRef]
11. Qiu, G.X.; Miao, D.J.; Wei, X.L.; Bai, C.; Li, X.M. Effect of MgO/Al_2O_3 and CaO/SiO_2 on the metallurgical properties of $CaO\text{-}SiO_2\text{-}Al_2O_3\text{-}MgO\text{-}TiO_2$ slag. *J. Non-Cryst. Solids* **2022**, *585*, 121545. [CrossRef]
12. Yan, Z.; Lv, X.; Zhang, J.; Qin, Y.; Bai, C. Influence of MgO, Al_2O_3 and CaO/SiO_2 on the viscosity of blast furnace type slag with high Al_2O_3 and 5%TiO_2. *Can. Metall. Quart.* **2016**, *55*, 186–194. [CrossRef]
13. Wang, C.; Zhang, J.; Jiao, K.; Liu, Z. Influence of basicity and MgO/Al_2O_3 ratio on the viscosity of blast furnace slags containing chloride. *Metall. Res. Technol.* **2017**, *114*, 395. [CrossRef]
14. Das, K.; Agrawal, A.; Reddy, A.S.; Ramna, R.V. FactSage studies to identify the optimum slag regime for blast furnace operation. *Trans. Indian Inst. Met.* **2021**, *74*, 419–428. [CrossRef]
15. Jiang, C.; Li, K.; Zhang, J.; Qin, Q.; Liu, Z.; Liang, W.; Sun, M.; Wang, Z. The effect of CaO(MgO) on the structure and properties of aluminosilicate system by molecular dynamics simulation. *J. Mol. Liq.* **2018**, *268*, 762–769. [CrossRef]
16. Jin, H.B.; Yang, S.Y.; Liu, H.; Chen, Y.; He, S.; Wang, Q. Effect of CaO partial substituted by BaO on structure of aluminotitanate melts by molecular dynamics simulation. *J. Non-Cryst. Solids* **2023**, *605*, 122160. [CrossRef]
17. Liu, W.G.; Zuo, H.B. Effect of MnO and CaO substitution for BaO on the viscosity and structure of $CaO\text{-}SiO_2\text{-}MgO\text{-}Al_2O_3\text{-}BaO\text{-}MnO$ slag. *J. Non-Cryst. Solids* **2021**, *567*, 120940. [CrossRef]
18. Bi, Z.S.; Li, K.J.; Jiang, C.H.; Zhang, J.L.; Ma, S.F. Effects of amphoteric oxide (Al_2O_3 and B_2O_3) on the structure and properties of SiO_2-CaO melts by molecular dynamics simulation. *J. Non-Cryst. Solids* **2021**, *559*, 120687. [CrossRef]
19. Lei, J.; Yang, W.; Sheng, G.Y.; Zhang, C.; Wu, T.; Wang, H.C. Effects of BaO Content and CaO/Al_2O_3 ratio on the properties and structure of aluminate slag. *Metall. Mater. Trans. B* **2022**, *53*, 2239–2247. [CrossRef]
20. Zhang, C.; Kong, Y.; Wu, T.; Bao, G.D.; Lei, J.; Wang, H.C. Effect of B_2O_3 on the structure and properties of aluminate slag. *Metall. Res. Technol.* **2022**, *119*, 507. [CrossRef]
21. Bo, W.; Jian, X.; Zhang, H.L.; Sun, S.; Feng, Z. Influence of MgO on calcium aluminate slag system with lower calcium. *Adv. Mater. Res.* **2014**, *3226*, 941–944. [CrossRef]
22. Qin, J.H.; Liu, W.G.; Wu, H.J.; Wang, J.; Xue, Q.; Zhao, H.; Zuo, H. A comprehensive investigation on the viscosity and structure of $CaO\text{-}SiO_2\text{-}Al_2O_3\text{-}MgO\text{-}BaO$ slag with different Al_2O_3/SiO_2 ratios. *J. Mol. Liq.* **2022**, *365*, 120060. [CrossRef]
23. Wang, W.; Dai, S.; Zhou, L.; Zhang, J.; Tian, W.; Xu, J. Viscosity and structure of $MgO\text{-}SiO_2$-based slag melt with varying B_2O_3 content. *Ceram. Int.* **2020**, *46*, 3631–3636. [CrossRef]
24. Chen, Z.W.; Meng, Z.; Liu, L.L.; Wang, H.; Sun, Y.; Wang, X. Structural and viscous insight into impact of MoO_3 on molten slags. *Metall. Mater. Trans. B* **2021**, *52*, 3730–3743. [CrossRef]
25. Liu Hao Qin, Y.L.; Yang, Y.H.; Zhang, Q.; Deng, N. Influence of Al_2O_3 content on the melting and fluidity of blast furnace type slag with low TiO_2 content. *J. Chem.* **2018**, *2018*, 9502304. [CrossRef]
26. Zhang, W.; He, F.; Xiao, Y.; Xie, M.; Xie, J.; Li, F.; Yang, H.; Li, Z. Structure, crystallization mechanism, and properties of glass ceramics from molten blast furnace slag with different B_2O_3/Al_2O_3. *Mater. Chem. Phys.* **2020**, *243*, 122664. [CrossRef]
27. Jin, Z.; Wang, B.; Liu, Z.; Yang, H.; Zou, M. Effects of Fe/SiO_2 ratio and MgO content on the viscous behaviors of the SiO_2-FeO-MgO-12 wt pct Fe_2O_3-8wt pct CaO-3 wt pct Al_2O_3 slag system. *Metall. Mater. Trans. B* **2022**, *53*, 902–915. [CrossRef]
28. Kong, W.G.; Liu, J.H.; Yu, Y.W.; Hou, X.M.; He, Z.J. Effect of $w(MgO)/w(Al_2O_3)$ ratio and basicity on microstructure and metallurgical properties of blast furnace slag. *J. Iron Steel Res. Int.* **2021**, *28*, 1223–1232. [CrossRef]
29. Yang, D.; Zhou, H.; Wang, J.; Pang, Z.; Pei, G.; Yan, Z.; Mao, H.; Qiu, G.; Lv, X. Influence of TiO_2 on viscosity, phase composition and structure of chromium-containing high-titanium blast furnace slag. *J. Mater. Res. Technol.* **2021**, *12*, 1615–1622. [CrossRef]
30. Feng, C.; Chu, M.S.; Tang, J.; Qin, J.; Li, F.; Liu, Z.G. Effects of MgO and TiO_2 on the viscous behaviors and phase compositions of titanium-bearing slag. *Int. J. Min. Met. Mater.* **2016**, *23*, 868–880. [CrossRef]

Disclaimer/Publisher's Note: The statements, opinions and data contained in all publications are solely those of the individual author(s) and contributor(s) and not of MDPI and/or the editor(s). MDPI and/or the editor(s) disclaim responsibility for any injury to people or property resulting from any ideas, methods, instructions or products referred to in the content.